

Biomechanical evaluation of an intramedullary nailing device by multibody analysis

G. Putame¹, M. Terzini¹, C. Bignardi¹, P. Costa², E. Zanetti³, A. Audenino¹

¹ Department of Mechanical and Aerospace Engineering, Politecnico di Torino, Torino, Italy

² Intrauma S.p.A, Rivoli (TO), Italy

³ Department of Engineering, University of Perugia, Perugia, Italy

Abstract — The present study investigates the suitability of the multibody method as alternative approach to the finite element method in order to evaluate biomechanical performances of a Marchetti-Vicenzi self-locking nail under dynamic loading. Torsional, compressive and bending dynamic loads were simulated. Results in terms of bone-device contact forces and device stiffness were obtained confirming and supporting issues observed in clinical reports.

Keywords — intramedullary nail, multibody analysis, biomechanics, bone fracture

I. INTRODUCTION

INTRAMEDULLARY nail fixation is a gold standard treatment for long bone diaphyseal fractures. Compared to interlocking nails constrained in the medullary canal through proximal and distal fixation screws, self-locking nails allow for reduced soft tissues injuries in the distal area thanks to expandable mechanisms. Although different self-locking mechanisms have been proposed, they still show limitations in terms of implant stability and reversibility. In order to predict the *in vivo* implant stability, static analysis using finite element method is generally adopted [1]-[3]. However, static analysis cannot describe interaction between bone and nail during dynamic loads. This study investigates the suitability of the numerical multibody analysis as alternative approach to evaluate biomechanical performance of an intramedullary self-locking nailing device under dynamic loads. In particular, a device derived from the Marchetti-Vicenzi nail was examined.

II. MATERIALS AND METHODS

A. Multibody approach

Two main critical aspects were identified in the model design: the former deal with the high number of contacts among model parts, the latter is related to the self-locking mechanism, which involves large deformations of its parts. In an attempt to reduce high computational costs due to the whole model complexity, a multibody approach was chosen. Numerical simulations were carried out using ADAMS/Solver software package (2017, MSC Software, Santa Ana, CA), which includes a native modelling object (i.e. finite element part) able to accurately solve large deformation cases [4].

B. Fracture model

A 3D standard model of the human femur was used to reproduce the physiological geometry of the medullary canal that surrounds the implanted device. In accordance with AO/OTA classification, a 32-A2 fracture was reproduced by removing a bone slice (1 mm thick) at 30° to the frontal body

axis. Therefore, the two obtained bone segments were modelled as two distinct rigid bodies. A density of 2000 kg/m³ was used for the osseous components.

C. Self-locking nailing device model

The Marchetti-Vicenzi nail consists of a hollow stub in which the proximal ends of six pre-curved wires are crimped together. The six pre-curved distal ends of the wires are free to expand in the medullary canal when the slider component, which initially keeps the six wires closed, is moved proximally over the axis nail (Fig. 1). Unlike other rigid parts of the model, wires were modelled as deformable cylinders. The selected material for all device parts was the stainless steel AISI 316 LVM with the following mechanical properties: Young's modulus 200 GPa, Poisson's ratio 0.3 and density 8000 kg/m³.

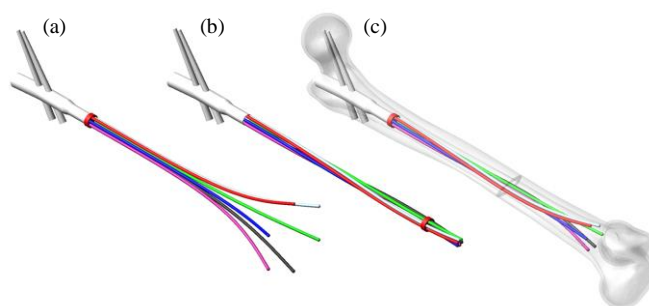


Figure 1. (a) Nail model at the beginning of the closing step; (b) Nail model at the end of the closing step; (c) Nail model at the end of the opening step inside the fractured femur model (slider at proximal position).

D. Simulation steps and loading conditions

Prior to loading, simulation involved two steps: first, the self-locking mechanism closure aimed at the mechanism preload (Fig. 1b); second, the self-locking mechanism opening in the medullary canal space (Fig. 1c). During the opening step, the slider was stopped in three different positions (namely distal, medial and proximal) along the longitudinal axis of the nail. Then, for each different longitudinal position of the slider, three types of dynamic loading conditions were simulated [5]: torsional, compressive and bending loads, which were sequentially applied to the distal bone segment as shown in Figure 2. It should be noted that four supporting cylinders were introduced in the model to simulate the four-point bending test. All dynamic loads were applied using a 0.25 Hz sinusoidal waveform. In detail, for the torsional load along the longitudinal axis of the femur, a maximal torsional moment of 500 N·mm was applied over 6 seconds. For the compressive load, a maximal axial force of 750 N was applied over 2 seconds. Finally, for the bending

load, a maximal downward force of 175 N was applied to each upper supporting cylinder. Contact force between each wire tip and the medullary canal surface were measured during the opening step. Displacement values were measured and post-processed by using MATLAB software (R2017a, MathWorks Inc., Natick, MA, USA) to obtain the model stiffness for each loading case and slider position.

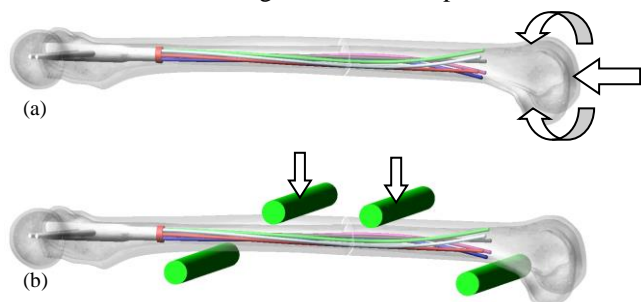


Figure 2. Models for compressive and torsional tests (a) and four-point bending test with four supporting cylinders (in green) (b). White arrows indicate applied forces and moments.

E. Model constraints

Four types of contact pairs were defined: wire-to-wire, wire-to-slider, wire-to-bone and bone-to-support. Last two contact pairs were assumed frictionless. No contact between proximal and distal bone segments was considered and a fixed joint was imposed between proximal bone segment and stub. To allow appropriate loading conditions, translations and rotations of the two bone segments were conveniently fixed or released in run-time. Besides, it should be specified that a spherical joint was imposed between each wire tip and the medullary canal surface when loading conditions were applied. Such an assumption was justified since the present study aimed at assessing the mechanical behaviour of the self-locking nail in relation to its opening arrangement in a physiologic-like geometry.

III. RESULTS AND DISCUSSION

In this section, results in terms of bone-device contact forces and mean stiffness for each studied loading case are presented and discussed. In Figure 3 contact forces between wire tips and bone are shown. Considering the measured tip penetration depths during contacts, contact pressure of 240 MPa on average was obtained. Such pressure values may be related to bone reabsorption or cracks, with a consequent loss of distal locking [3]. Therefore, high contact pressure might explain cracks propagation and wire protrusions observed in previous clinical reports [6] [7]. As can be seen in Table 1, stiffness is lower for internal rotation than for external one. This is due to the winding direction that wires acquire during the closing step. Bending stiffness, obtained as applied force versus displacement for each upper cylinder, resulted slightly higher when the slider was at its distal position. Although results suggest that the device stiffness always increases when the slider is at its distal position, compressive stiffness value for the proximal case is higher than expected. This is due to the occurrence of diaphyseal contacts between the wire stems and the canal during the compression.

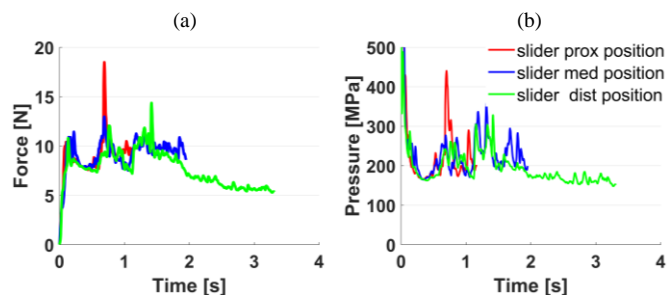


Figure 3. Contact force (a) and pressure (b) between wire tips and intramedullary canal during the opening phase.

TABLE I
TORSIONAL, BENDING, COMPRESSIVE STIFFNESS AND DISPLACEMENTS

TORSIONAL LOADING CONDITION				
Slider position	External rotation		Internal rotation	
	Max Disp. (°)	Mean Stiff. (Nmm/°)	Max Disp. (°)	Mean Stiff. (Nmm/°)
Distal	11.7	38.4	15.5	36.7
Medial	27.2	28.6	20.6	26.6
Proximal	28.2	37.0	13.1	33.4
BENDING LOADING CONDITION				
Slider position	Proximal cylinder		Distal cylinder	
	Max Disp. (mm)	Mean Stiff. (N/mm)	Max Disp. (mm)	Mean Stiff. (N/mm)
Distal	11.7	10.7	10.5	12.3
Medial	15.1	8.9	15.2	9.8
Proximal	15.6	8.6	15.4	8.7
COMPRESSIVE LOADING CONDITION				
Slider position	Max Disp. (mm)		Mean Stiff. (N/mm)	
Distal	0.5		1479.9	
Medial	1.1		517.8	
Proximal	0.8		736.7	

IV. CONCLUSION

Even though the present study is based on a specific nailing device, the findings suggest that the multibody method may be a valid alternative approach to the finite element method in order to assess the biomechanical performance of complex models that involves large deformations and many contacts.

REFERENCES

- [1] D. Ivanov, Y. Barabash and A. Barabash, "A numerical comparative analysis of ChM and Fixation nails for diaphyseal femur fractures", in *Acta of Bioengineering and Biomechanics*, vol. 18, pp. 73-81, 2016
- [2] D. Ivanov, A. Barabash and Y. Barabash, "Preclinical biomechanics of a new intramedullary nail for femoral diaphyseal fractures", in *Russian Open Medical Journal*, vol. 4, 2015
- [3] F. Giudice, G. La Rosa, T. Russo and R. Varsalona, "Evaluation and improvement of the efficiency of the Seidel humeral nail by numerical-experimental analysis of the bone-implant contact", in *Medical Engineering & Physics*, vol. 28, pp. 682-693, 2006
- [4] MSC ADAMS/View software user guide, "Getting started with FE Parts", 2017
- [5] G. Wang, T. Pan, X. Peng and J. Wang, "A new intramedullary nailing device for the treatment of femoral shaft fractures: A biomechanical study," in *Clinical Biomechanics*, vol. 23, pp. 315-312, 2008
- [6] S. Madan, R. Natarajan, S. Walsh and C. Blakeway, "The Marchetti-Vicenzi nail. A DGH experience", in *Injury, Int. J. Care Injured*, vol. 34, pp. 346-348, 2003
- [7] A. Ruffilli, F. Traina, F. Pilla, D. Fenga and C. Faldini, "Marchetti Vicenzi elastic retrograde nail in the treatment of humeral shaft fractures: review of the current literature", in *Musculoskelet Surg*, vol. 99, pp. 201-209, 2015